https://doi.org/10.5194/essd-2021-245
Preprint. Discussion started: 26 July 2021

Open Access Earth System Science Data Discussions

Water masses distribution offshore the Sabrina Coast (East Antarctica)

Bensi Manuel[1], Kovačević Vedrana[1], Donda Federica[1], O'Brien Philip E.[2], Armbrecht Linda[3], Armand Leanne K.[4]

[1] National Institute of Oceanography and Applied Geophysics (OGS), Trieste, 34010, Italy;
[2] Department of Environmental Sciences, Macquarie University, Sydney, Australia;
[3]Australian Centre for Ancient DNA, Department of Ecology & Evolutionary Biology, School of Biological Sciences, The University of Adelaide, South Australia 5005, Australia;
[4]Australian National University, Canberra, Australia;

Correspondence to: M. Bensi (mbensi@inogs.it)

Abstract

Current glacier melt rates in West Antarctica substantially exceed those around the East Antarctic margin. The exception is Wilkes Land where, e.g., Totten Glacier, underwent significant retreat between 2000 and 2012, underlining its sensitivity to climate change. This process is strongly influenced by ocean dynamics, which in turn changes in accordance with the evolution of the ice caps. Here, we present oceanographic data (temperature, salinity, density, dissolved oxygen) collected for the first time offshore the Sabrina Coast (East Antarctica), from the continental shelf break to ca 3000 m depth during austral summer 2017.

The main water masses are identified by analysing thermohaline properties: the Antarctic Surface Water with $\theta > -1.5$ °C and $S < 34.2$ ($\sigma_\theta < 27.55$ kg m^{-3}), the Winter Water with $-1.92 < \theta < -1.75$ °C and $34.0 < S < 34.5$ ($27.55 < \sigma_\theta < 27.7$ kg m^{-3}), the modified Circumpolar Deep Water with $\theta > 0$ °C and $S > 34.5$ ($\sigma_\theta > 27.7$ kg m^{-3}), and Antarctic Bottom Water with $-0.50 < \theta < 0$ °C and $34.63 < S < 34.67$ ($27.83 < \sigma_\theta < 27.85$). The latter in this region is a mixture of dense waters originating from the Ross Sea and Adélie Land continental shelves, and is affected by the mixing process they undergo as they move westward along the Antarctic margin and interact with the locally formed dense waters, and with the warmer and saltier Circumpolar Deep Water.

The spatial distribution of water masses offshore the Sabrina Coast also appears to be strongly linked with the complex morpho-bathymetry of the slope and rise area, supporting the hypothesis that downslope processes contribute to shaping the architecture of the distal portion of the continental margin.

Short summary (plain text)

The Totten Glacier (Sabrina Coast, East Antarctica) has undergone significant retreat in recent years, underlining its sensitivity to climate change and its potential contribution to global sea-level rise. The melting process is strongly influenced by ocean dynamics and the spatial distribution of water masses appears to be linked to the complex morpho-bathymetry of the area, supporting the hypothesis that downwelling processes contribute to shaping the architecture of the continental margin.

https://doi.org/10.5194/essd-2021-245
Preprint. Discussion started: 26 July 2021

Open Access Earth System Science Data Discussions

1 Introduction

[1] Polar regions are key components of Earth's climate system and are particularly sensitive to ongoing climate change effects induced by anthropogenic pressures. It has been estimated that the full melting of all Antarctic ice has a sea level equivalent (SLE) of ~58 m (Fretwell et al., 2013).

Understanding Earth's climate processes as well as their future projections strongly depend on the constant collection and interpretation of long-term scientific data and palaeoclimatic records. Therefore, studying long-term records from these regions is key (e.g., Masson-Delmotte et al., 2013) to have a more complete understanding of the region's past climate variability (e.g., Escutia et al., 2019). Within this frame, quantifying sea-level rise associated with global warming is crucial, and the accuracy of such quantifications ultimately depends on our knowledge of the response of polar regions to global warming. In fact, there is still significant uncertainty in estimates around sea-level rise, as Church et al. (2013) reported in the IPCC AR5 Sea Level Chapter. They delineate that significant challenges remain in understanding and predicting processes related to the dynamic response of Antarctic marine-terminal glaciers and marine sectors. The Antarctic ice sheet response to current climate forcing can be elucidated by examining how the ice sheet had behaved in response to similar climate forcings in the past. In spite of the significant effort in putting the estimates together, the IPCC report expresses only medium confidence in estimating the contribution of Antarctic ice melt to sea levels during the last major warm episode, e.g. the Last Interglacial period, ca 129k to 116k years ago (Masson-Delmotte et al., 2013).

Marine processes change in accordance with the evolution of the ice caps and vice versa, especially in those areas where glaciers are grounded below sea level. This condition occurs not only in West Antarctica, but also in several portions of East Antarctica (e.g., Adelie Land, Rignot et al., 2011), including the Sabrina Coast. Here, the Totten Glacier is largely grounded below sea level and hence susceptible to marine ice sheet instabilities (Pritchard et al., 2009; Aitken et al., 2014). Totten Glacier is the downstream end of the vast Aurora subglacial basin, most of which is below sea level (Roberts et al., 2011; Young et al., 2011) and exposed to temperatures up to 3 °C above the ice shelves' melting point (Rignot et al., 2013). The Aurora subglacial basin today also hosts an active subglacial hydrological system that drains basal meltwater to the ocean (Wright et al., 2012).

[2] According to Silvano et al. (2018), while relatively warm waters (> 0°C) flood the continental shelves in West Antarctica driving rapid basal melt of ice shelves, the ice shelves in East Antarctica experience relatively low rates of basal melt because they are influenced by cooler waters (< 0°C). However, the Totten Glacier is an exception, since the melting rates of this glacier and of the nearby Moscow University ice shelf (MUIS) are among the fastest in the East Antarctic Ice Sheets (about 5-7 Gt/y and 3 Gt/y respectively, from the '80s; Khazendar et al., 2013; Li et al., 2016; Mohajerani et al., 2018; Rignot et al., 2019). They are likely enhanced by incursions of relatively warm modified Circumpolar Deep Water (mCDW) to the glacier grounding line (Rintoul et al., 2016; Silvano et al., 2016; 2017), indicating high vulnerability to rapid collapse. Rignot et al. (2019) reported that Totten Glacier holds an ice volume that translates into a sea-level equivalent of 3.85 m. The mCDW on the Sabrina Coast continental shelf is usually characterized by a temperature around −0.4 °C and a salinity around 34.5–34.6, and comprises the bottom layer of

https://doi.org/10.5194/essd-2021-245
Preprint. Discussion started: 26 July 2021

the water column. This appears to be different from other coastal areas of East Antarctica, where the bottom layer is usually occupied by colder and denser Shelf Water (Bindoff et al., 2000; Greenbaum et al., 2015). Studies of rapidly retreating outlet glaciers in the Amundsen Sea have shown a major role of the mCDW in transporting warm water from the deep ocean onto the shelf, leading to enhanced glacier melting (Jenkins et al., 2010, Smith et al., 2011, Pritchard et al., 2012). This process has also been suggested as a possible cause for the rapid melting of Totten Glacier (Williams et al., 2011, Pritchard et al., 2012), but other mechanisms have been also suggested. Pritchard et al. (2012) invoked that changes in the circum-Antarctic wind field and its effects on upwelling around the continent cause the rapid basal melting of the Totten Glacier. Also, Khazendar et al. (2013) and Gwyther et al. (2014) have argued that this enhanced melting is the result of complex interactions between oceanic and shelf water masses at the base of the ice. In particular, they suggested that the ice melting is strongly modulated by cold High Salinity Shelf Water formed in polynyas to the east of the Totten Glacier and channelled by local bathymetry to the base of the glacier. These studies rely heavily on satellite observations and bathymetry of the regions, e.g. the 1 km horizontal grid resolution obtained through the General Bathymetric Chart of the Oceans (GEBCO) used for oceanographic models (Gwyther et al., 2014). The GEBCO grid has 2 ship tracks in the critical 150 km by 200 km area seaward of the Totten Glacier, meaning that most of the grid is a "best guess".

[3] The Antarctic ice sheet nucleated in the higher elevations of the Gamburtsev Mountains and first reached the ocean near the Sabrina Coast and Prydz Bay (Huybrechts 1993, DeConto & Pollard 2003). Marine-terminating glaciers existed at the Sabrina Coast by the early-middle Eocene (ca. 56–41 Ma), implying the occurrence of ice caps before the emplacement of continental-scale ice sheets (Gulick et al., 2017). The first preserved evidence of grounded ice on the Sabrina Coast shelf is suggested to be Late Eocene in age (ca. 38 Ma; Gulick et al., 2017). The climate evolution of the Wilkes Land margin, and thus of the Sabrina Coast, from the pre-glacial Era to the present time comprises three main key periods: i) pre-glacial conditions (Phase 1 reported in Donda et al., 2007); ii) growth and development of a polythermal, highly dynamic ice sheet (Phases 2 and 3 in Donda et al., 2007), and iii) transition to polar conditions (Phase 4 in Donda et al., 2007). This overall picture is well supported by several Antarctic and sub-Antarctic stratigraphic records, e.g., the Deep Sea Drilling Program Leg 28, Cape Roberts Drilling Project, Ocean Drilling Program Legs 119, 188, and 189 and International Ocean Discovery Program Leg 318 (Donda et al., 2020). Compared to other areas, the Sabrina Coast seismostratigraphy suggests that downslope processes contributed to shaping the distal margin architecture even during its latest development stages (i.e., Phase 4), when glacial meltwater-related fluxes were able to erode and deliver sediments to the rise area (Donda et al., 2020). The continental slope and rise of the Sabrina Coast reveal remarkable differences between the eastern and western areas, as also highlighted by the present-day bathymetry (Fig. 1). The western sector is shallower and characterized by the presence of two prominent NE-SW trending ridges, separated by a low sinuosity narrow submarine canyon flanked with terraces. Armand et al. (2018) described the eastern facing ridge slopes as smooth seafloor with significant evidence of mass movement (e.g., slump scars and debris runout fields), while the westward facing slopes are gullied terrain (with a gully depth range of up to 15 m). In fact, the associated canyon is not receiving a high proportion of downslope turbidity currents,

https://doi.org/10.5194/essd-2021-245
Preprint. Discussion started: 26 July 2021

rather being fed by slumping on the adjacent ridge flanks (O'Brien et al., 2020). The eastern ridge was reported as having a lower slope than the western ridge, and being dominated by slump scars. The eastern sector, instead, is characterized by a complex network of erosional channels and it is shaped by dendritic canyons, which meander and bend sharply to then join less sinuous main channels, the floors of which contain terraces and closed depressions (O'Brien et al., 2020). The ridges between canyons are clearly tied to their adjoining canyons and formed by westward advection of fine sediment lofted from turbidity currents and deposition of pelagic sediment (O'Brien et al., 2020). The western and the eastern areas are separated by a broad depression linked with one of the dendritic canyons near the lower slope. The upper slope consists of a smooth to gullied apron, downslope of which the canyon heads begin. The shelf break occurs at depths of 480 - 510 m.

[4] This paper aims at describing the thermohaline structures from the continental shelf break to about 3000 m depth identified for the first time offshore Sabrina coast, by analysing physical oceanographic data collected in 2017 during a multidisciplinary expedition (see below).

https://doi.org/10.5194/essd-2021-245
Preprint. Discussion started: 26 July 2021

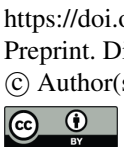

Open Access Earth System Science Data Discussions

2 The oceanographic dataset: instrumentation and data processing

Oceanographic data presented in this paper were collected offshore the Sabrina coast, between 113°E and 122°E and 66° S and 64°S (Fig. 1) during the marine geoscience expedition "Interactions of the Totten Glacier with the Southern Ocean through multiple glacial cycles" (IN2017-V01) (see Armand et al., 2018). This expedition took place between 14 January and 7 March 2017 on board the Australian Marine National Facility (MNF) Research Vessel *Investigator*.

.

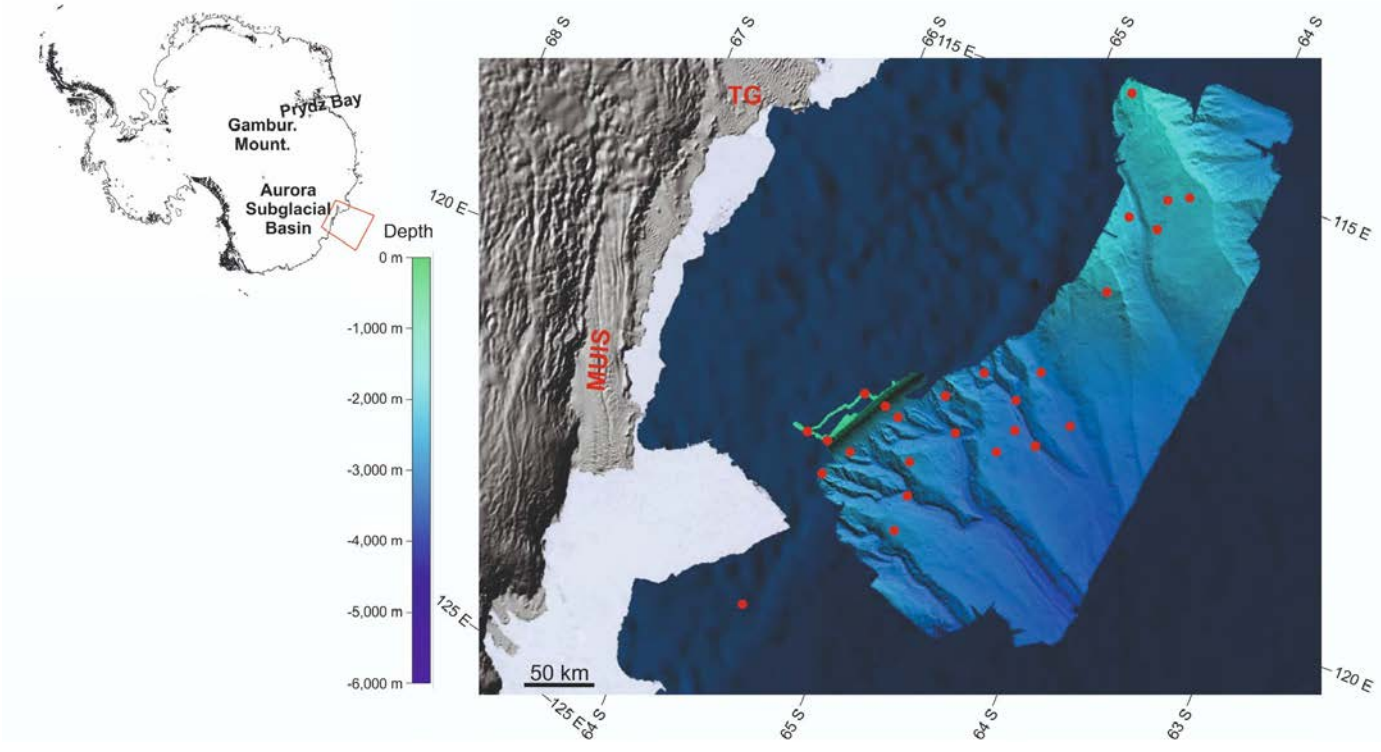

Figure 1. Sabrina Seafloor Survey area. *The high resolution bathymetry obtained from multibeam data acquired during the IN2017-V01 cruise (from O'Brien et al., 2020) is superimposed over the lower resolution bathymetry from the International Bathymetric Chart of the Southern Ocean. On land, the terrain map comes from the Reference Elevation Model of Antarctica (REMA, Howat et al., 2019). The colorbar on the left refers to the high resolution multibeam bathymetry.*

[1] We take into account 31 Conductivity-Temperature-Depth (CTD) vertical profiles (labeled 1-11, 13-23, 25-33) acquired in the study region (Fig. 2) using a Seabird SBE911 CTD equipped with 24 niskin bottles (OceanTest Equipment Inc. Florida; 12-L capacity each one, mounted on the rosette sampler), sensors for measuring dissolved oxygen concentration (DO, SBE43), and altimeter (PA500). The Commonwealth Scientific and Industrial Research Organisation (CSIRO) supplied calibration factors that were used to compute pressure, temperature, and conductivity/salinity values. Data were subjected to automated quality control (QC) to remove spikes and out-of-range values (see https://www.cmar.csiro.au/data/reporting/get_file.cfm?eov_pub_id=1512, last

https://doi.org/10.5194/essd-2021-245
Preprint. Discussion started: 26 July 2021

access on July 06, 2021). Particular attention was taken in the post processing phase to remove spikes and out of range values, while maintaining true data features. An additional filter was applied to the data to evaluate the median and standard deviation of the conductivity over a moving window. This allowed us to detect extreme changes in the sensor values characteristic of the noise induced by spikes. The conductivity calibration was based on two deployment groupings, due to sensor changes during the voyage, and it was based upon the comparison between conductivity data obtained from CTD and water samples (104 of the total of 151 water samples taken during deployments). The final calibration for casts 1-13 from the secondary sensor had a standard deviation (std) of 0.001 psu, within our target of 'better than 0.002 psu', while the final calibration for casts 14-33 from the secondary sensor had a std of 0.002 psu. Water samples were also collected and used to compute new estimates of DO calibration coefficients, obtained by applying a linear regression. A single calibration group from each sensor was used with the associated SBE43 up-cast data. The DO calibration had a std of 0.85911 µM with a good agreement between the sensor and bottle data. Based on the results obtained from the calibration procedure, the final dataset was obtained after 1 dbar binned averaged data from the secondary sensors (primary sensor for DO). Note that seven CTD profiles (casts 1, 2, 11, 13, 14, 15, and 18, in Fig. 1) stopped before reaching the seafloor (between 200 and 700 m, e.g., for testing the new sensor settings). Potential temperature (θ, °C) and potential density anomaly (σ_θ, kg m^{-3}, referred to 0 dbar), and neutral density (γ^n, kg m^{-3}) were calculated using the toolbox TEOS-10 (http://www.teos-10.org/software.htm). We use σ_θ when considering the property distribution in the upper 500 m, and where the specific σ_θ values determine and delimit specific water masses within the upper layers. However, the depth range of our study area is wide, and σ_θ errors augment with depth, therefore γ^n for the entire vertical range along vertical sections is used instead to depict the property distributions. Neutral density (γ^n) is a function of temperature, salinity, pressure, latitude and longitude, where the reference level is slightly adjusted at each point to compensate for the nonlinearity of the equation of state, hence it can be considered a locally-referenced potential density. Some figures were created using Ocean Data View (ODV; Schlitzer, 2021). More detailed information on instrumentation and quality control procedure are available at https://www.cmar.csiro.au/data/trawler/survey_details.cfm?survey=IN2017_V01 (last access on July 06, 2021).

Finally, satellite images (MODIS Corrected Reflectance imagery) indicate an area of open water in the sea ice cover, in the vicinity of Totten Glacier and MUIS, with an extension of about 6.7 km^2 (Fig. 2b,c) during the entire period of the oceanographic cruise. Satellite images used in this work are freely available from the NASA Worldview application (https://worldview.earthdata.nasa.gov), part of the NASA Earth Observing System Data. The spatial imagery resolution is 250 m, and the temporal resolution is daily.

https://doi.org/10.5194/essd-2021-245
Preprint. Discussion started: 26 July 2021

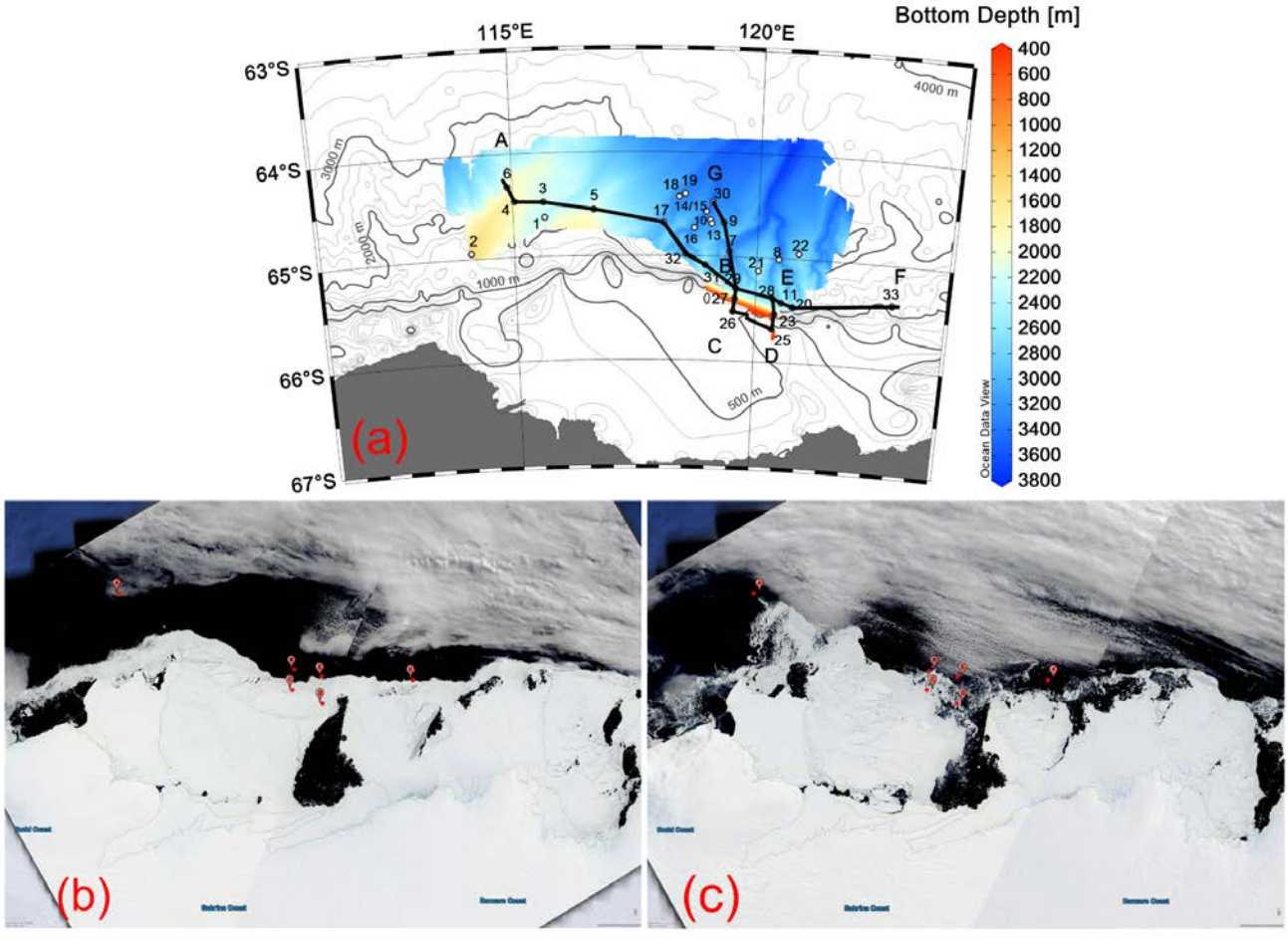

153
154
155 ***Figure 2*** *- CTD stations map and color-coded high resolution bathymetry collected during the* IN2017-V01 *cruise (from O'Brien*
156 *et al., 2020), superimposed over the International Bathymetric Chart of the Southern Ocean (contour lines). Positions A, B, C, D,*
157 *E, F, and G denote along-slope and cross-slope sections (a). The same positions A-F (red dots) along the ice edge are*
158 *superimposed on satellite images (MODIS Corrected Reflectance imagery freely available from*
159 *https://worldview.earthdata.nasa.gov/) taken on 23 January (b) and 26 February 2017 (c), which show the temporal evolution of*
160 *the sea ice extension in the study region at the beginning and at the end of the IN2017-V01 cruise.*

https://doi.org/10.5194/essd-2021-245
Preprint. Discussion started: 26 July 2021

Open Access Earth System Science Data Discussions

3 Thermohaline patterns in the study region

3.1 Typical water masses

CTD casts are distributed over the continental slope and rise, offshore the area delimited by Totten Glacier and MUIS (Fig. 2). The main water masses are identified by analysing their θ-S (and DO) properties (Fig. 3) and classified according to Silvano et al. (2017, 2020). They are: Antarctic Surface Water (**AASW**) with θ > -1.5 °C and S < 34.2 (σ_θ < 27.55), Winter Water (**WW**) with -1.92 < θ < -1.75 and 34.0 < S < 34.5 (27.55 < σ_θ < *27.7* kg m^{-3}), and **mCDW**, with θ □ 0 °C and S > 34.5 (σ_θ > *27.7* kg m^{-3}). The AASW and WW are the most ventilated and therefore have the highest dissolved oxygen values. Acquired data do not reveal the presence of water with characteristics either of Ice Shelf Water (**ISW,** θ < -1.92 °C, *S* < 34.5, 27.55 < σ_θ < *27.7* kg m^{-3}) or Dense Shelf Water (**DSW,** θ < -1.92 °C, *S* > 34.5, σ_θ > *27.7* kg m^{-3}). In particular, the former is usually found close to the two ice shelves, and the latter forms within the polynyas, because of the intense cooling and brine rejection processes that can take place there. AASW comprises a wide range of both temperature and salinity. It is warm due to summer heating, and fresh due to glacial meltwater. WW is a homogeneous layer formed through convection over the shelf during previous winter, and mCDW is a relatively warm and salty water mass that can access the shelf and the water cavities below the ice shelves causing ice melting (Greenbaum et al., 2015). The thermohaline properties associated with the densest waters are attributed to the Antarctic Bottom Water (**AABW,** with -0.50< θ <0 °C, 34.63< S <34.67, 27.83< σ_θ <27.85 kg m^{-3}). The AABW in this part of the Australian Antarctic Basin (AAB) is a mixture of the local and remote dense waters, namely the Adélie Land Bottom Water (**ALBW**) and Ross Sea Bottom Water (**RSBW**, see e.g., Silvano et al., 2020), both of which have distinct characteristics in their source regions (Thomas et al., 2020). The most recent typical θ-S average values encountered during 2018 in the AAB (Thomas et al., 2020) were -0.599 °C/34.704 for the RSBW, and -0.632 °C/ 34.619 for the ALBW. We argue that these endmember values are representative also for the conditions encountered in 2017. However, thermohaline properties reported for the AABW in 2017 in our study area (Fig. 3) were slightly higher (~ +0.10 °C and +0.05 for θ and S, respectively) than those referred to the mentioned endmembers, reflecting the mixing process that bottom waters experience as they move westwards along the Antarctic margin.

https://doi.org/10.5194/essd-2021-245
Preprint. Discussion started: 26 July 2021

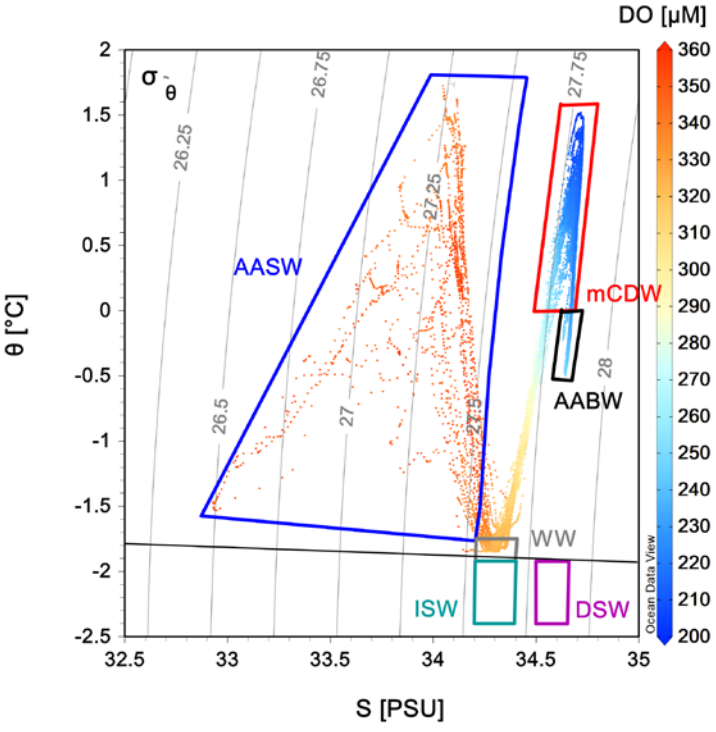

Figure 3 *- θ-S diagram with colours referring to dissolved oxygen concentration (colorbar on the right). Characterization of the principal water masses, based on the continental shelf data according to Silvano et al. (2017, 2020): AASW - Antarctic surface water, WW - winter water, mCDW - modified Circumpolar Deep Water, AABW- Antarctic bottom water, the densest water spreading westwards from the Ross Sea (with properties captured at 150°E), ISW - Ice Shelf Water and DSW - Dense Shelf Water are not present Black solid line corresponds to the surface freezing temperature.*

3.2 Vertical distribution of the hydrographic properties

To describe thermohaline properties in the study area and in proximity of the sea ice edge, we consider a zonal section (West-Est) running almost parallel to the continental slope, extending from station 6 to station 25 (see Fig. 2), combined with two short cross-slope segments in correspondence of the shelf break. An overall distribution of θ, S, DO concentration, and neutral density (Fig. 4) indicates well defined layers of AASW, WW, and mCDW. AASW is situated in the relatively shallow surface layer (0 -50 m depth), but with a wide range of varying temperature and salinity. Cold, fresh, and relatively uniform in temperature and salinity, Winter Water lays beneath within the upper 400 m with larger thickness over the slope and shelf break. Beneath 400 m depth, warm and salty mCDW occupies the largest portion of the water column, decreasing its temperature and salinity approaching the shelf break (between positions C and D). There, it spreads over the continental shelf.

https://doi.org/10.5194/essd-2021-245
Preprint. Discussion started: 26 July 2021

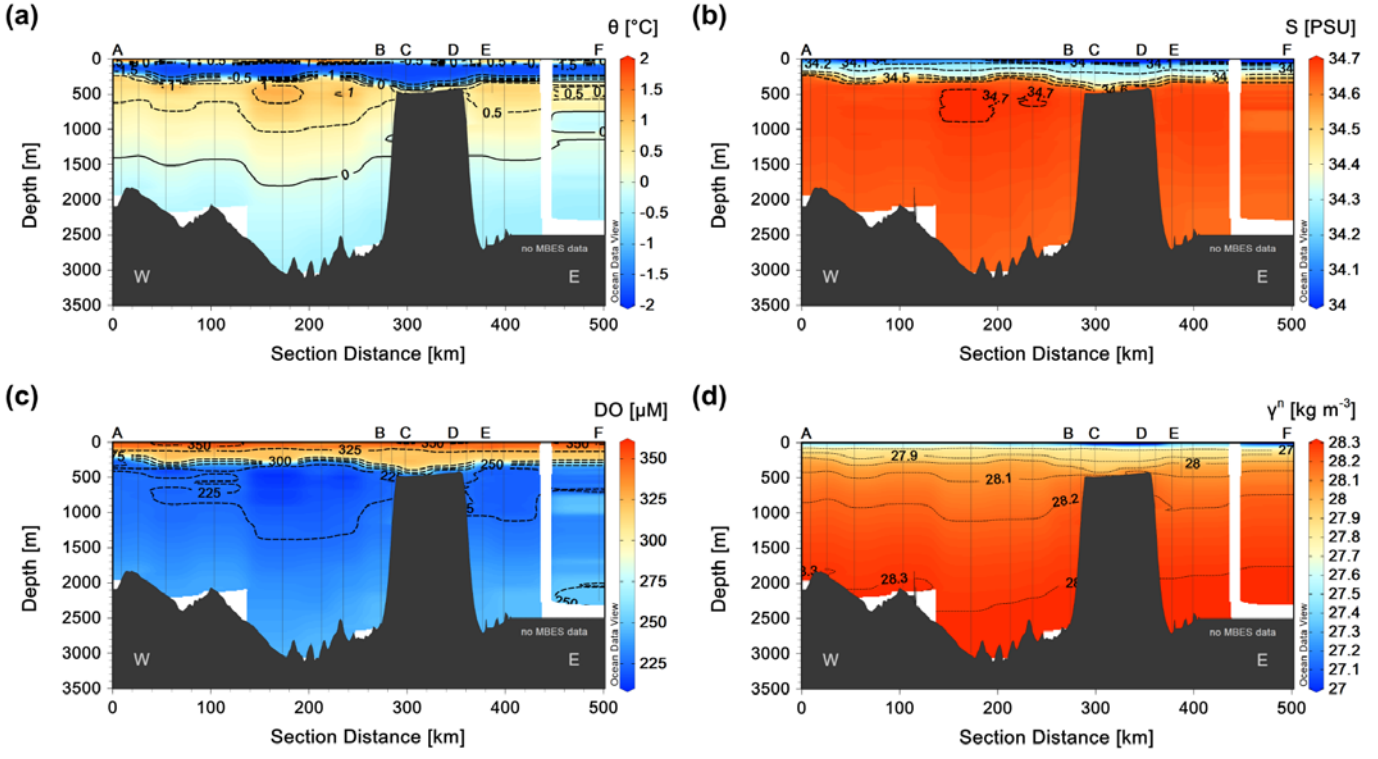

Figure 4 *- Along-slope transect (ABCDEF) against distance with two across-slope segments, BC and DE (see Fig. 3). Vertical distribution of θ (a), S (b), DO concentration (c), and neutral density (d) over the entire depth range.*

A closer look into the upper 500 m layer (Fig. 5) reveals a well oxygenated AASW. Its temperature and salinity decrease at the shelf break (area BCDE), probably due to the influence of cold and fresh ice melting water coming from the continental shelf (see Fig. 2b,c for the evolution of sea ice in January-February 2017). The portion of the water column occupied by Winter Water, approximately between 50 m and 400 m depth, is cold (-1.5°C < θ < -0.5 °C), relatively fresh (S < 34.45), and well oxygenated (DO >300 µM). The largest thickness of Winter Water corresponds to the area approaching the continental shelf break (BCDE, water depths between 400 and 500 m), suggesting that such water was spreading from the continental shelf (Silvano et al., 2017).

https://doi.org/10.5194/essd-2021-245
Preprint. Discussion started: 26 July 2021

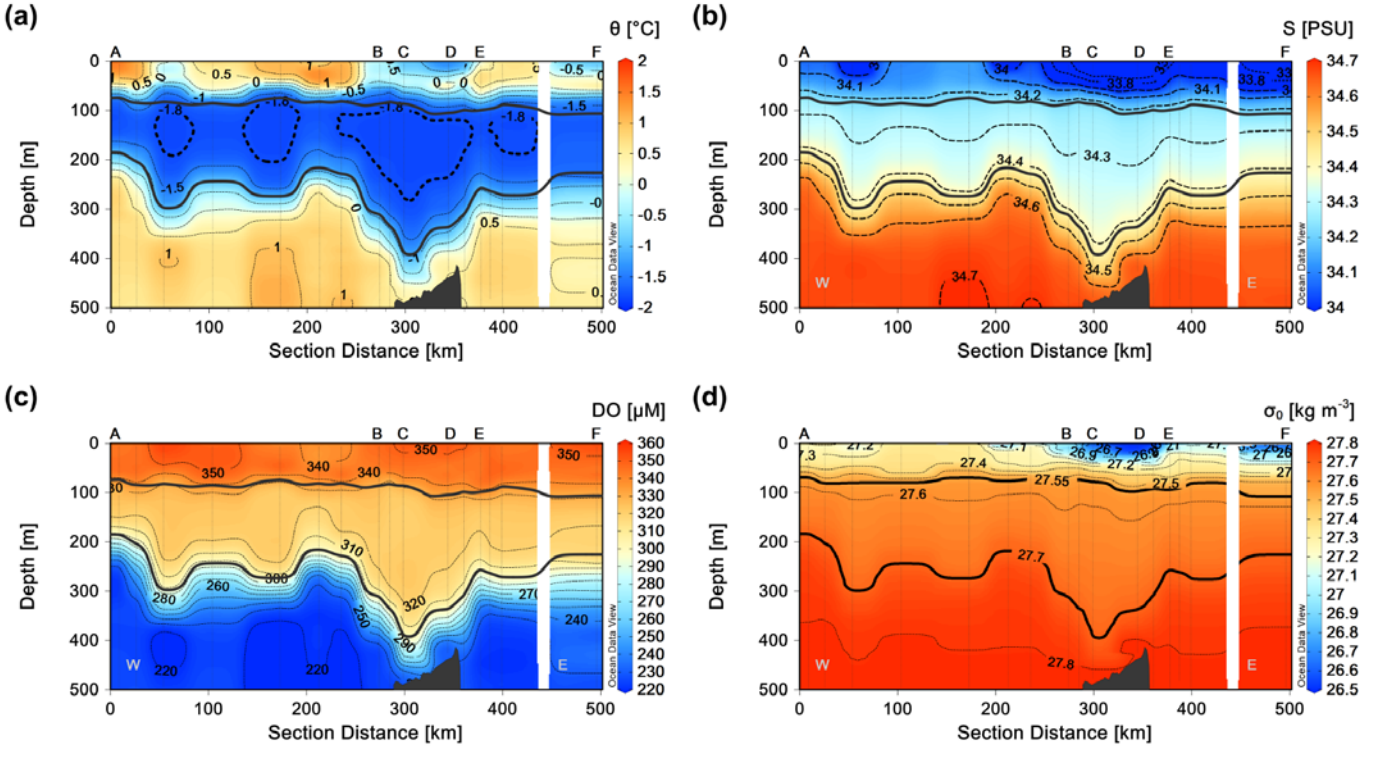

Figure 5 *- Along-slope transect (between positions A and F shown in figure 2) against distance. Vertical distribution of θ (a), S (b), DO concentration (c), and σ_θ referring to 0 dbar (d) in the upper 500 m. Thick black lines in each panel indicate isopycnals 27.55 and 27.70 kg m^{-3}, delimiting the layer occupied by WW (defined according to Silvano et al., 2017).*

From 500 m down to the continental slope and rise area, to depths greater than 3000 m, both temperature and salinity progressively decrease. Below 1500 m (Fig. 6), in particular, cold waters have temperatures ranging from 0 °C to almost -0.5 °C near the bottom. The lowest temperature values (-0.479 °C) are recorded in the easternmost part of the zonal transect, along with relatively low salinity (38.638–38.640), and high oxygen (up to 248-250 μM) especially in the easternmost part of the section. The densest waters lay in the depressions/canyons/troughs between 118° and 119°E (neutral density 28.325 kg m^{-3}). Despite the relatively large distance among CTD stations, the sections of the thermohaline properties and dissolved oxygen concentration reveal that, close to the bottom, in correspondence of the canyons and rugged bottom morphology (e.g., near positions B and E in Fig. 6) there are signals of possible pathways of dense waters likely originated on the shelf or within the polynya area. The high resolution of the neutral density isolines makes it possible to detect how the isopycnals, and all other properties, follow the bottom morphology (Fig. 6).

https://doi.org/10.5194/essd-2021-245
Preprint. Discussion started: 26 July 2021

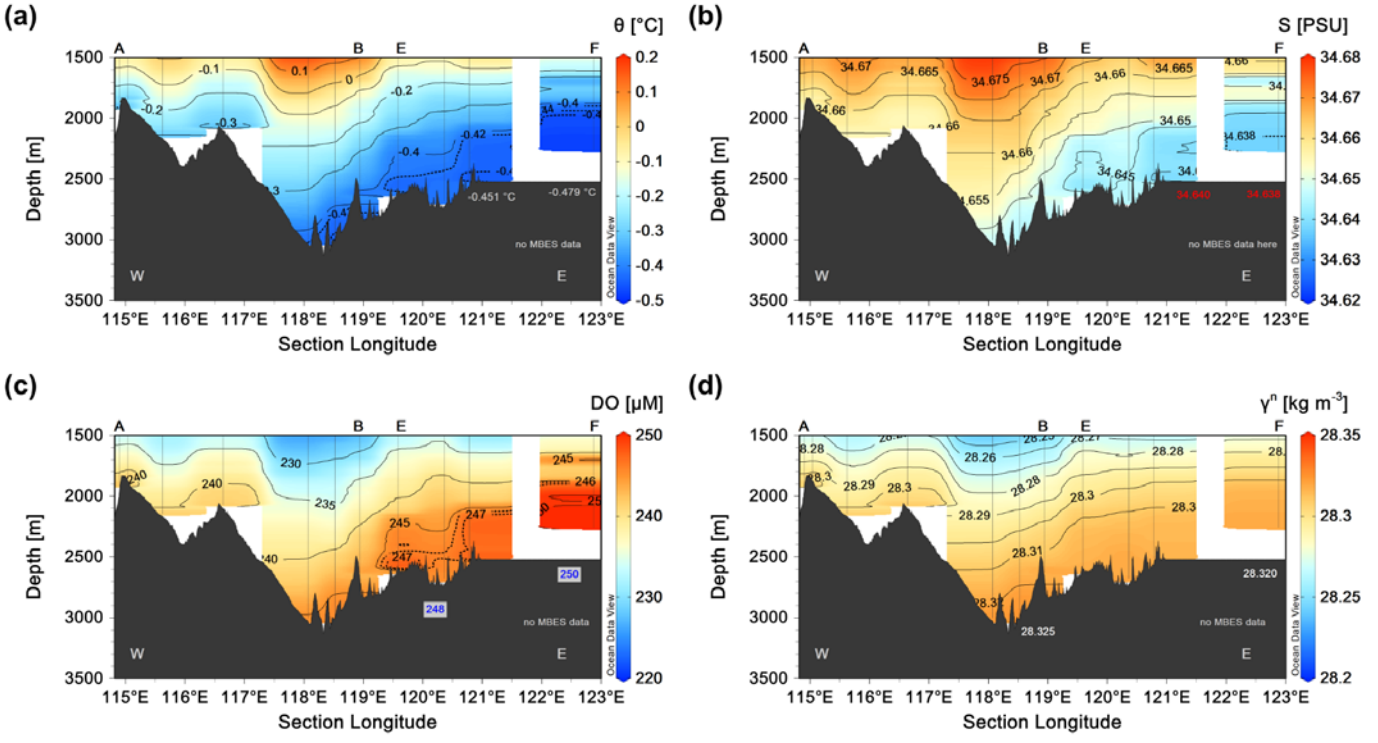

Figure 6 *- Along-slope transect (positions ABEF of figure 2) against the geographical longitude (see Fig. 3). Vertical distribution of θ (a), S (b), DO concentration (c), and neutral density (d) in the deep depth range (1500 m – bottom). The isoline steps are chosen to make evident small changes of the hydrographic properties near the bottom where waters are the coldest, the freshest, the densest, as well as rich in dissolved oxygen content.*

Patches of the deepest and densest waters have properties that may be attributed to those of the AABW (Fig. 4), not excluding the hypothesis that these dense patches may result from the contribution of dense, cold, and relatively fresh waters originating from the continental shelf. Indeed, they could be produced by mixing among mCDW, dense waters formed within the polynya, and maybe also ice shelf basal melting water. The spreading of such water out of the continental shelf area can give origin to the density driven flows that descending within the canyons along the continental slope can contribute to shape the observed sea-floor morphologies described by O'Brien et al (2020).

To better identify the distribution of the water masses between the continental shelf and the open sea area we draw a S-N across-slope section.

https://doi.org/10.5194/essd-2021-245
Preprint. Discussion started: 26 July 2021

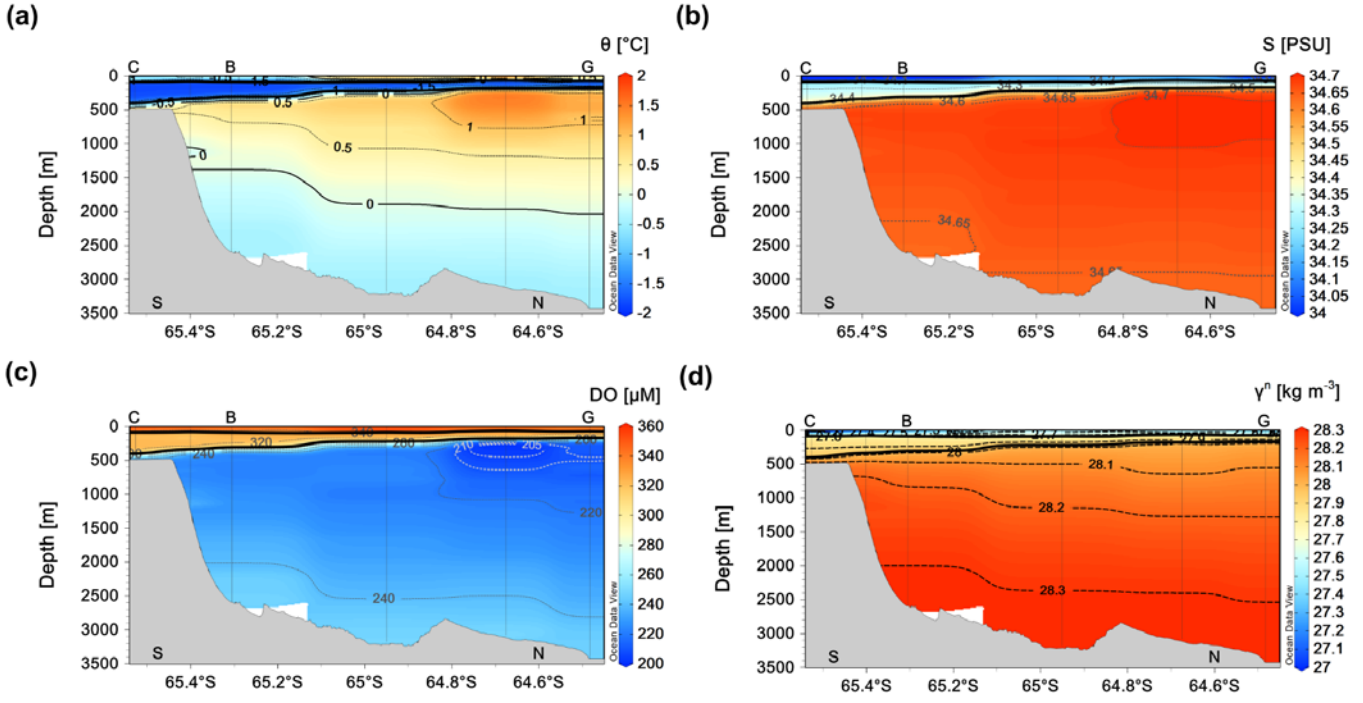

Figure 7 *- Across-slope transect (positions CBG of figure 2) against the geographical latitude (see Fig. 3). Vertical distribution of θ (a), S (b), DO concentration (c), and neutral density (d) over the entire depth range. Isopycnals of 27.55 and 27.7 kg m^{-3} are shown in all panels (thick black lines), delimiting WW (according to Silvano et al., 2017).*

In fact, the across-slope section (positions CBG, see Fig. 7) illustrates a progressive thinning of the Winter Water layer from the shelf break toward the open sea. This contrasts with the thick core layer of mCDW in the open sea area, where it peaks in θ and S and reaches the minimum in DO content between 64.6 °N and 64.8 °N. The layer occupied by mCDW progressively narrows in the opposite direction toward the shelf break, where it also becomes less warm and less salty. There, the mCDW tongue protrudes toward the shelf beneath the WW. On the continental slope, at approximately 1100 m depth, a slight temperature decrease (Fig. 7a) hints at the eventual downslope flow of cold waters originating from the shelf. However, the coarse spacing between CTD stations precludes defining a finer thermohaline structure. The deep and near-bottom seawater properties shown in Fig. 8 better illustrate how the isopycnals and associated thermohaline properties, along with the DO content, align with the morphology of the sea floor. There, coherent changes in θ, S, and DO point out at a cold, relatively fresh, and oxygenated bottom layer, approximately 400-500 m thick, leaning on the continental slope and rise. Its well delimited characteristics fade away from 64.6 °S northward.

https://doi.org/10.5194/essd-2021-245
Preprint. Discussion started: 26 July 2021

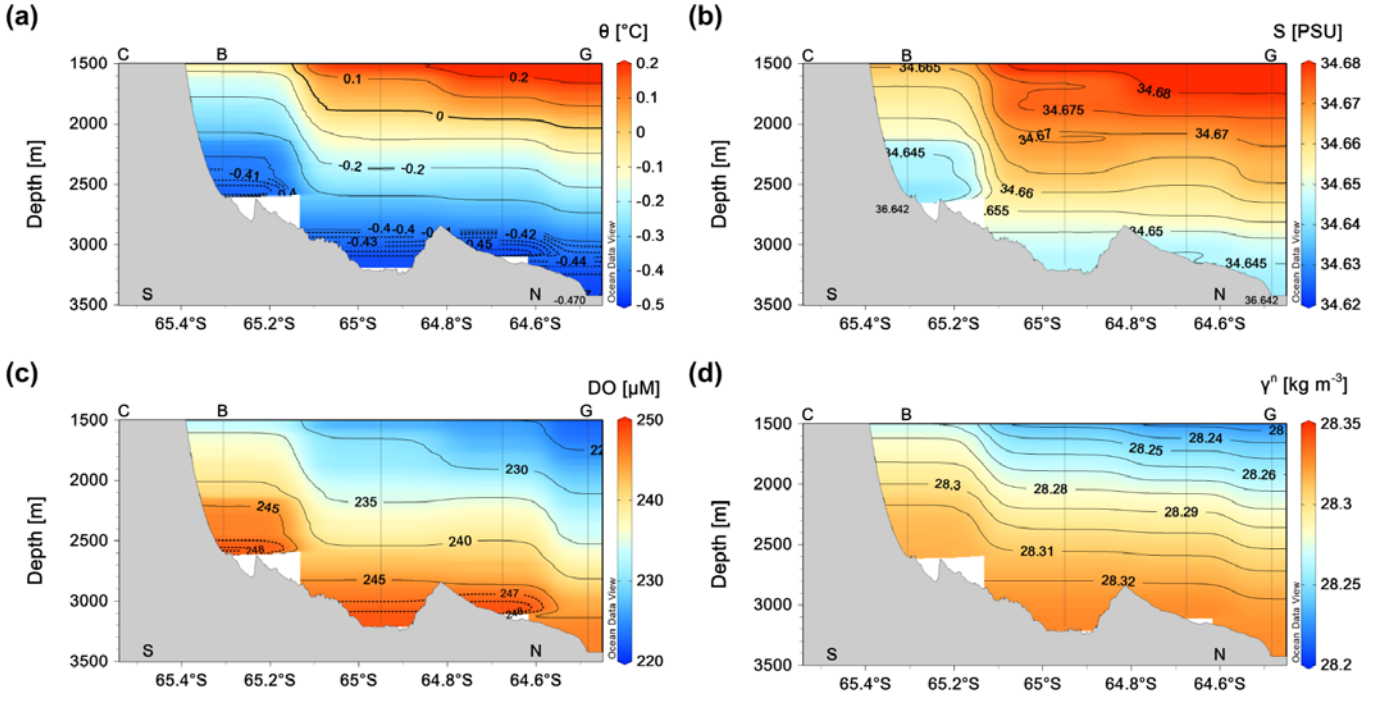

Figure 8 *- Same as figure 7 but with a zoom into the 1500 m - bottom layer. The isoline steps are chosen to make evident small changes of the hydrographic properties near the bottom where waters are the coldest, the freshest, the densest, as well as rich in dissolved oxygen content.*

3.3 Spatial distribution of the hydrographic properties

The horizontal distribution of the thermohaline properties near the surface (Fig. 9a, c, e, g) over the study area shows how similar thermohaline properties group into bands almost parallel to the isobaths, matching with the shelf, shelf-break and slope, as well as with the continental rise, and gradually or abruptly change from the shelf toward the open sea. From the shelf area (bottom depths smaller than 500 m), low-density (low θ and S), DO-rich waters, approach the shelf break where they mix with the saltier and warmer mCDW. The strongest signal of the shelf waters is visible along 120.5 °E. Over the shelf break and slope, there is a more pronounced mixing with the open sea waters favoured also by the complex bathymetry. In the northernmost offshore portion of the study region a marked influence of mCDW is highlighted by higher θ and S values, up to 2.0° C and 34.2, respectively.

https://doi.org/10.5194/essd-2021-245
Preprint. Discussion started: 26 July 2021

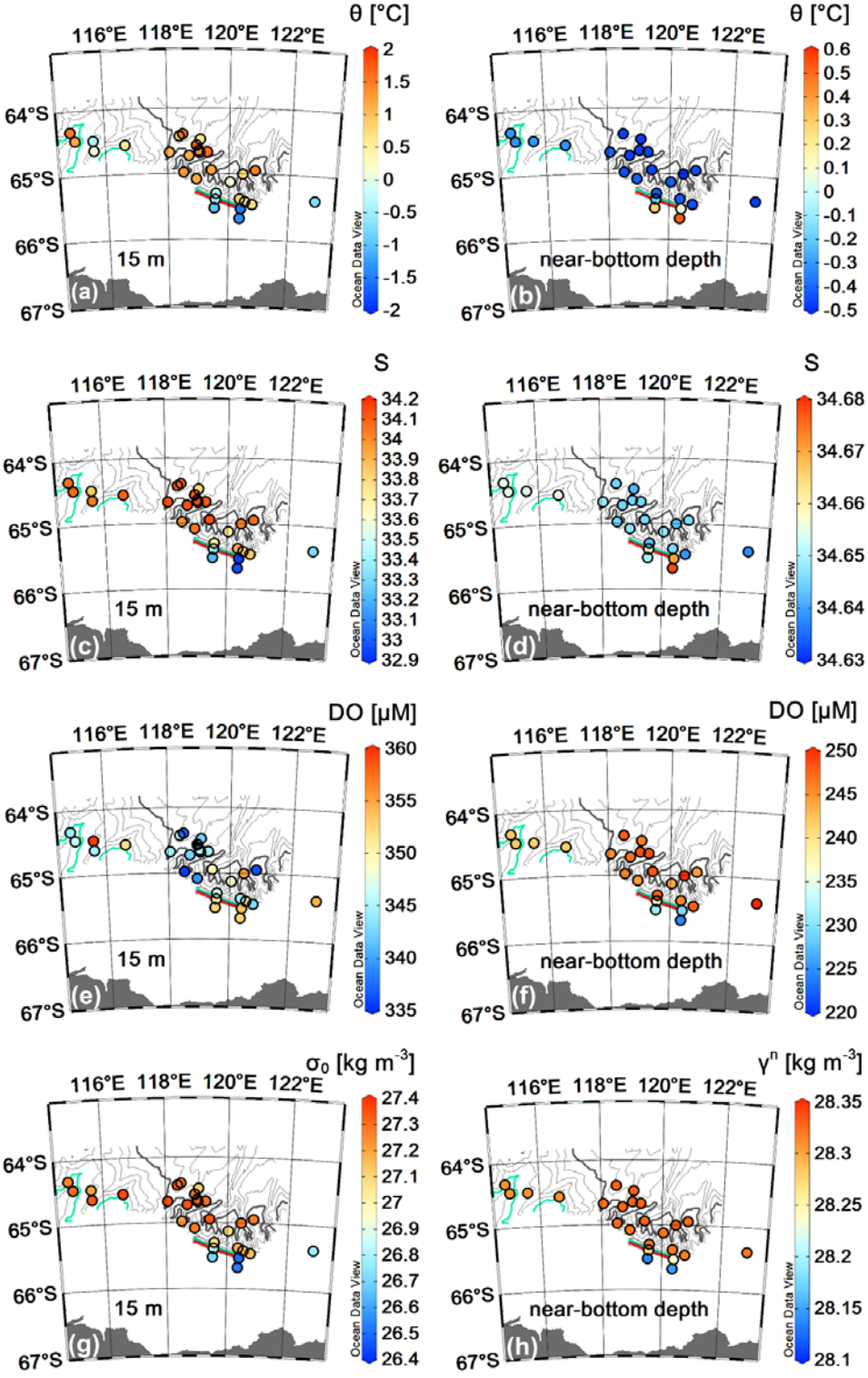

https://doi.org/10.5194/essd-2021-245
Preprint. Discussion started: 26 July 2021

***Figure 9** - Near-surface (15 m depth) θ (a), S (c), DO content (e), and σ_θ (g) and near-bottom θ (b), S (d), DO content (f), and neutral density γ^n (h). The background bathymetry consists of isobaths (thin black curves) every 200 m obtained from MBES data acquired during the 2017 campaign; thick lines indicate isobaths at 1000 m (red), 2000 m (cyan), and 3000 m (gray).*

Close to the bottom over the shelf break, maxima θ and S values (about 0.5°C and 34.678, respectively) were registered at the southernmost station 25 (on the shelf break, at 420 m depth). These large near-bottom values reflect the mCDW impinging on the slope beneath the cold and fresh waters resulting from ice melting (around 120 °E). Overall, in the westernmost part of the study area (115°E - 117°E) at depths around 2000 m, the bottom layer was occupied by waters with θ around -0.30°C and S around 34.65-34.66, hence slightly warmer and saltier (and less dense) than bottom waters found in the central part of the study area, where the bottom depth is larger (see Fig. 9b,d and Fig. 6). The fact that bottom waters in the western sector also have lower DO values suggests that this area, where maximum depth slightly exceeds 2000 m depth, is most influenced by mCDW, which protrudes even more southward within the Totten Trough reaching the front of the Totten Glacier, as highlighted by Silvano et al. (2017).

4 Summary and conclusions

Here we present oceanographic data (temperature, salinity, density, dissolved oxygen) collected for the first time offshore the Sabrina coast (Antarctica), between 113°E and 122°E and 66° S and 64°S (Fig. 1). The spatial distribution of the water masses, described mainly according to their θ/S properties, appears to be linked to the complex morpho-bathymetric setting of the study area, supporting the hypothesis that downslope processes contribute to shaping the distal margin architecture (e.g., Donda et al., 2020). Small variations of the thermohaline properties in the 400–500 m thick layer above the seabed revealed that in correspondence of the canyons there are signals of dense waters with low θ and S values (-0.445 °C and 38.638 – 38.640, respectively), and relatively high DO (240-250 μM) values. This suggests that such waters originate or have a contribution from dense waters that come from the shelf area and flow along the continental slope. Descending dense water plumes fill the deep layer, possibly mixing with the AABW originating from the combination of RSBW and ALBW. These outcomes would support the (occasional) occurrence of density-driven currents in this region, which could contribute, on the one side, to shape the present-day, erosional character of the deeply-incised canyons and, on the other side, to redistribute the different water masses (i.e., AASW, WW, and mCDW) offshore the continental shelf beyond the shelf edge, favouring their mixing. At the same time, our data revealed that the westernmost and deepest part of the study area appears to be occupied by waters that are less cold and saltier, as well as less oxygenated, than those occupying the bottom layer in the central part. This asymmetric distribution of deep waters offshore the Sabrina coast seems to be an effect generated by the particular morphology of the seabed. In addition, ocean currents and associated processes (along-slope flow, tides, internal waves, downslope density-driven currents) that involve local water masses may be different in the two deep zones. This implies that the accumulation of locally formed dense waters, as well as their

https://doi.org/10.5194/essd-2021-245
Preprint. Discussion started: 26 July 2021

downward flow, may occur mainly in the central part of the study area and contribute to modify deep waters of remote origin (e.g., from the Ross Sea and Adélie Land).

The campaign was conducted during summer, when rapidly changing sea-ice conditions influenced the near-surface layers, hence affected by ice-melt waters. The complex interaction of the continental shelf, slope and rise dynamics in this area is certainly challenging, suggesting the importance of learning more about oceanographic dynamics during both winter and summer seasons. In particular, the possibility of acquiring high temporal resolution data, especially during the winter period (e.g., by using long-term in situ observatories), could help in the understanding of the oceanographic processes that have contributed to shape the distal margin architecture and have influenced the evolution of the ice sheet.

5 Data availability

All data used in this work are archived in the enduring CSIRO Data Access Portal, https://data.csiro.au. Metadata records are made publicly available at http://www.marlin.csiro.au. Processed data and data products are, instead, publicly available through Data Trawler http://www.cmar.csiro.au/data/trawler/index.cfm, the MNF web data access tool http://www.cmar.csiro.au/data/underway/, and/or from national or world data centers most suitable for the dissemination of particular data types. All metadata entries should list this requested acknowledgment statement where the data are presented or published (Armand et al., 2018).

Declaration of Competing Interest

The authors declare that they have no known competing financial interests or personal relationships that could have appeared to influence the work reported in this paper.

Acknowledgements

We thank the Marine National Facility, the IN2017-V01 scientific party, led by the Chief Scientists L.K. Armand and P. O'Brien, MNF support staff and ASP crew members led by Capt. M. Watson for their help and support on board the RV Investigator. This Project was supported through funding from the Australian Government's Australian Antarctic Science Grant Program (AAS #4333) and the Australian Research Council's Discovery Projects funding scheme (DP170100557). We would like also to acknowledge the financial support of the Italian National Antarctic Research Program (Programma Nazionale di Ricerche in Antartide, PNRA) that funded the participation of the Italian team to the cruise through the project TYTAN (Totten Glacier dYnamics and Southern Ocean circulation impact on deposiTional processes since the mid-lAte CeNozoic) led by F. Donda.

https://doi.org/10.5194/essd-2021-245
Preprint. Discussion started: 26 July 2021

Open Access Earth System Science Data Discussions

Author contribution

M.B., V.K., and F.D. conceived and wrote the article. M.B. and V.K. processed the data used to prepare the figures and performed the analyses. F.D. led the TYTAN project, L.K.A. and P.O. led the IN2017-V01 scientific cruise. L.A. contributed to collect experimental data and participated in writing the text. All authors contributed to the discussion and revision of the manuscript.

https://doi.org/10.5194/essd-2021-245
Preprint. Discussion started: 26 July 2021

6 References

Armand L. K, O'Brien P. E., and On-board Scientific Party: Interactions of the Totten Glacier with the Southern Ocean through multiple glacial cycles (IN2017-V01), Post-survey report, Research School of Earth Sciences, Australian National University, Canberra, http://dx.doi.org/10.4225/13/5acea64c48693, 2018.

Bindoff, N. L., Rosenberg, M. A., and Warner, M. J.: On the circulation and water masses over the Antarctic continental slope and rise between 80 and 150°E, Deep-Sea Res PT II, 47(12), 2299–2326, doi:10.1016/S0967-0645(00)00038-2, 2000.

De Conto, R. M. and Pollard, D.: Rapid Cenozoic glaciation of Antarctica induced by declining atmospheric CO2. Nature, 421, 245–249, https://doi.org/10.1038/nature012902003.

Donda, F., Brancolini, G., O'Brien, P. E., De Santis, L., and Escutia, C.: Sedimentary processes in the Wilkes Land margin: a record of Cenozoic East Antarctic Ice Sheet evolution. J Geol Soc London, 164, 243-256, https://doi.org/10.1144/0016-76492004-159 2007.

Donda, F., Leitchenkov, G., Brancolini, G., Romeo, R., De Santis, L., Escutia, C., O'Brien, P. E., Armand, L., Caburlotto, A., and Cotterle, D.The influence of the Totten Glacier on the Late Cenozoic sedimentary record. Antarctic Science, doi:10.1017/S0954102020000188, 2020.

Escutia, C., DeConto, R.M., Dunbar, R. De Santis, L., Shevenell, A. and Naish, T.: Keeping an eye on Antarctic Ice Sheet stability. Oceanography 32(1):32–46, https://doi.org/10.5670/ oceanog.2019.117, 2019.

Fretwell, P., Pritchard, H.D., Vaughan, D.G., Bamber, J.L., Barrand, N.E., Bell, R., Bianchi C., Bingham, R.G., Blankenship, D.D., Casassa, G., and others. 2013. Bedmap2: Improved ice bed, surface and thickness datasets for Antarctica. Cryosphere 7:375–393, https://doi.org/10.5194/tc-7-375-2013.

Greenbaum, J. S., Blankenship, D. D., Young, D. A., Richter, T. G., Roberts, J. L., Aitken, A. R. A., Legresy, B., Schroeder, D. M., Warner, R. C., van Ommen, T. D., and Siegert, M. J.: Ocean access to a cavity beneath Totten Glacier in East Antarctica, Nat Geosci, 8(4), 294–298, doi:10.1038/ngeo2388, 2015.

Gulick, S., Shevenell, A., Montelli, A., Fernandez, R., Smith, C., Warny, S., Bohaty, S. M., Sjunneskog, C., Leventer, A., Frederick, B., and Blankenship, D. B: Initiation and long-term stability of the East Antarctic Ice Sheet in the Aurora Basin, Nature, 552, 225-241, doi: 10.1038/nature25026, 2020.

Gwyther, D. E., Galton-Fenzi, B. K., Hunter, J. R., and Roberts, J. L.: Simulated melt rates for the Totten and Dalton ice shelves, Ocean Science, 10(3), 267–279, doi:https://doi.org/10.5194/os-10-267-2014, 2014.

Howat, I. M., Porter, C., Smith, B. E., Noh, M.-J., and Morin, P.: The Reference Elevation Model of Antarctica, The Cryosphere, 13, 665-674, https://doi.org/10.5194/tc-13-665-2019, 2019.

Huybrechts, P.: Glaciological modelling of the late Cenozoic East Antarctic Ice Sheet: stability or dynamism? Geografiska Annaler Series A - Physical Geography, 4, 221–238, https://doi.org/10.1080/04353676.1993.11880395, 1993.

Khazendar, A., Schodlok, M. P., Fenty, I., Ligtenberg, S. R. M., Rignot, E., and van den Broeke, M. R.: Observed thinning of

Totten Glacier is linked to coastal polynya variability, Nat Commun, 4(1), 2857, doi:10.1038/ncomms3857, 2013.

Li, X., Rignot , E., Morlighem, M., Mouginot, J., and Scheuchl, B.: Grounding line retreat of Totten Glacier, East Antarctica, 1996 to 2013, Geophys Res Lett, 42(19), 8049-8056, doi:10.1002/2015GL065701, 2015.

Masson-Delmotte, V., Schulz, M., Abe-Ouchi, A., Beer, J., Ganopolski, A., González Rouco, J.F., Jansen, E., Lambeck, K., Luterbacher, J., Naish, T., Osborn, T., Otto-Bliesner, B., Quinn, T., Ramesh, R., Rojas, M., Shao, X., and Timmermann, A.: Information from Paleoclimate Archives. In: Climate Change 2013: The Physical Science Basis. Contribution of Working Group I to the Fifth Assessment Report of the Intergovernmental Panel on Climate Change [Stocker, T.F., D. Qin, G.-K. Plattner, M. Tignor, S.K. Allen, J. Boschung, A. Nauels, Y. Xia, V. Bex and P.M. Midgley (eds.)]. Cambridge University Press, Cambridge, United Kingdom and New York, NY, USA, 2013

Miles, B. W., Stokes, C. R. and Jamieson, S. S.: Pan–ice-sheet glacier terminus change in East Antarctica reveals sensitivity of Wilkes Land to sea-ice changes. Science advances, 2(5), p.e1501350. doi:10.1126/sciadv.1501350, 2016.

Mohajerani, Y., Velicogna, I., and Rignot, E.: Mass Loss of Totten and Moscow University Glaciers, East Antarctica, Using Regionally Optimized GRACE Mascons, Geophys Res Lett 45.14 7010-7018. doi: 10.1029/2018GL078173, 2018.

O'Brien, P. E. Post, A. L., Edwards, S., Martin, T. Caburlotto, Donda, F., Leitchenkov, G., Romeo, R., Duffy, M., Evangelinos, D., Holder, L., Leventer, A., López-Quirós, A., Opdyke, B. N., and Armand, L. K: Continental slope and rise geomorphology seaward of the Totten Glacier, East Antarctica (112ºE-122ºE), Mar Geol, 427, 106221, https://doi.org/10.1016/j.margeo.2020.106221, 2020.

Rignot, E., Mouginot, J., and Scheuchl, B.: Antarctic grounding line mapping from differential satellite radar interferometry, 38, https://doi.org/10.1029/2011GL047109, 2011.

Rignot, E., Jacobs, S., Mouginot, J., and Scheuchl, B.: Ice Shelf Melting Around Antarctica. Science, 341, 266-270. doi:10.1126/science.1235798, 2013.

Rignot, E., Mouginot, J., Scheuchl, B., van den Broeke, M., and Morlighem, M.: Four decades of Antarctic Ice Sheet mass balance from 1979–2017. Proceedings of the National Academy of Sciences, 116(4), 1095-1103. DOI: 10.1073/pnas.1812883116, 2019.

Rintoul, S. R., Silvano, A., Pena-Molino, B., van Wijk, E., Rosenberg, M., Greenbaum, J. S., and Blankenship, D. D.: Ocean heat drives rapid basal melt of the Totten Ice Shelf. Science Advances, 2, 12, e1 601610, DOI:10.1126/sciadv.1601610, 2016.

Roberts, J. L., Warner, R. C., Young, D., Wright, A., Van Ommen, T. D., Blankenship, D. D., Siegert, M., Young, N. W., Tabacco, I. E., Foieri, A., Passerini, A., Zirizzotti, A., and Frezzotti, M.: Refining broad-scale sub-glacial morphology of Aurora Subglacial Basin, East Antarctica derived by an ice-dynamic-based interpolation scheme. The Cryosphere Discussion, 5, 655-684, 2011.

Schlitzer, Reiner, Ocean Data View, odv.awi.de, 2021.

https://doi.org/10.5194/essd-2021-245
Preprint. Discussion started: 26 July 2021

Silvano, A., Rintoul, S. R., and Herraiz-Borreguero, L.: Ocean-Ice Shelf Interaction in East Antarctica, Oceanography, 29(4), 130–143, 2016.

Silvano, A., Rintoul, S. R., Peña-Molino, B., and Williams, G. D.: Distribution of water masses and meltwater on the continental shelf near the Totten and Moscow University ice shelves, J Geophys Res-Oceans, 122(3), 2050–2068, doi:10.1002/2016JC012115, 2017.

Silvano, A., Foppert, A., Rintoul, S. R., Holland, P. R., Tamura, T., Kimura, N., Castagno, P., Falco, P., Budillon, G., Haumann, F. A., Naveira Garabato, A. C., and Macdonald, A.: Recent recovery of Antarctic Bottom Water formation in the Ross Sea driven by climate anomalies, Nature Geoscience, 13, 780-786, doi: 10.1038/s41561-020-00655-3, 2020.

Thomas, G., Purkey, S. G., Roemmich, D., Foppert, A., Rintoul, S. R.: Spatial variability of Antarctic bottom water in the Australian Antarctic Basin from 2018–2020 captured by Deep Argo. Geophysical Research Letters, 47, e2020GL089467. https://doi.org/10.1029/2020GL089467, 2020.

Wright, A. Silvano, A., Rintoul, S. R., Peña-Molino, B., Hobbs, W. R., Wijk, E. van, Aoki, S., Tamura, T., and Williams, G. D.: Freshening by glacial meltwater enhances melting of ice shelves and reduces formation of Antarctic Bottom Water, Science Advances, 4(4), eaap9467, doi:10.1126/sciadv.aap9467, 2018.

P., Young, D. A., Roberts, J. L., Schroeder, D. M., Bamber, J. L., Dowdeswell, J. A., Young, N. W., Le Brocq, A. M., Warner, R. C., Payne, A. J., Blankenship, D. D., van Ommen, T. D., and Siegert, M. J.: Evidence of a hydrological connection between the ice divide and ice sheet margin in the Aurora Subglacial Basin, East Antarctica. J Geophys Res, 117, F01033, doi:10.1029/2011JF002066, 2012.

Young, D. A., Wright, A. P., Roberts, J. L., Warner, R. C., Young, N. W., Greenbaum, J. S., Schroeder, D. M., Holt, J. W., Sugden, D. E., Blankenship, D. D., Van Ommen, T. D., and Seigert, M. J.: A dynamic early East Antarctic Ice Sheet suggested by ice covered fjord landscapes, Nature, 474, 72-75, https://doi.org/10.1038/nature10114, 2011.